Parameter Extraction for Behavioral Model of Permanent Magnet Synchronous Machine in Field Weakening Operation Mode

Jonathan Smith[1], Thomas Wenninger[1], Helmut Didar Joseph[1], Thorsten Koch[2], Wen Soong[3], Nesimi Ertugrul[3], Carsten Markgraf[1], and Alexander Frey*[1]
[1]Augsburg University of Applied Sciences, Augsburg, Germany, [2]COMSOL Multiphysics GmbH, Goettingen, Germany, [3]The University of Adelaide, Adelaide, Australia

*Corresponding author: An der Hochschule 1, 86161 Augsburg, Germany, alexander.frey@hs-augsburg.de

Abstract: In this work, COMSOL is used to extract electrical PMSM parameters required for a behavioral model. Using the COMSOL *Rotating Machinery, Magnetic* application mode enables efficient model setup. A procedure is described showing how the *d*- and *q*-axis motor inductances are obtained. In addition, the voltage constant related to the motional e.m.f. is determined. These parameters are essential for implementing motor control. Moreover, to maximize the power density, a system design approach for the motor, motor control, inverter and gear is required and the reported simulations help to minimize the costs for hardware realization.

Keywords: electrical machines, PMSM, field-weakening, rotating machinery

1. Introduction

1.1 Motivation

In 2010, the Formula Student Electric (FSE) was introduced as a student design competition for battery electric driven race vehicles [1].

A competitive power train requires careful selection of the motor and gearing in conjunction with the control scheme. To optimize the performance, the "Starkstrom-Augsburg e.V." FSE-team [2] has started to custom design these components. The specification of the motor and gear are interdependent and are additionally influenced by the control scheme (cf. Sec. 1.2). Several engine parameters are necessary for the control implementation, which are only available once the motor design has been finalised. Thus an iterative design approach is required. The situation calls for simulation of the motor behavior to achieve good system performance and to minimize cost for hardware realization. In the past years, several papers have been published on how to use COMSOL for simulating different aspects of electric machines [3,4,5].

1.2 Electrical motor parameters

The permanent magnet synchronous machine (PMSM) offers high power density as required for the traction drive. The mechanical power P is given by:

$$P = T\omega_{mech} \quad (1)$$

with ω_{mech} being the mechanical rotational speed. The motor torque T follows from [6]:

$$T = \frac{3p}{2}\left(\Psi_{PM} i_q + \left(L_d - L_q\right) i_q i_d\right). \quad (2)$$

In Eq. 2, p is the number of pole pairs (cf. Sec. 2.1) and i is the current. The subscripts d and q indicate the *d*- and *q*-axis, respectively.

To calculate the torque, the *d*-axis flux linkage from the permanent magnets Ψ_{PM} and the inductances L_d and L_q are required. To illustrate the significance of these three important parameters, some motor behavior basics are reviewed with reference to the PMSM phasor diagram shown in Fig 1.

At the base speed $\omega_{mech,b} = \omega_{el,b}/p$, the situation is displayed in Fig. 1a. Along the *q*-axis the voltage V_p related to the motional e.m.f. and the ohmic voltage drop across the coil resistance R sum together. The voltage along the *d*-axis relates to the *q*-axis reactance. The terminal voltage phasor is shown in red, and its magnitude is shown to have reached the maximum value set by the voltage supply (dotted circle).

Operating the motor with higher speed $\omega_{mech} > \omega_{mech,b}$ requires field weakening [7,8] as displayed in Fig. 1b. By applying a negative i_d current, the voltage phasor can be kept within the allowed range that is limited by the available DC link voltage. The benefit of field weakening operation for the torque-speed characteristic is obvious from Fig. 2.

In this work, COMSOL is used to extract L_d and L_q and the voltage constant which is closely related to Ψ_{PM} (cf. Fig. 1, Sec. 3.3).

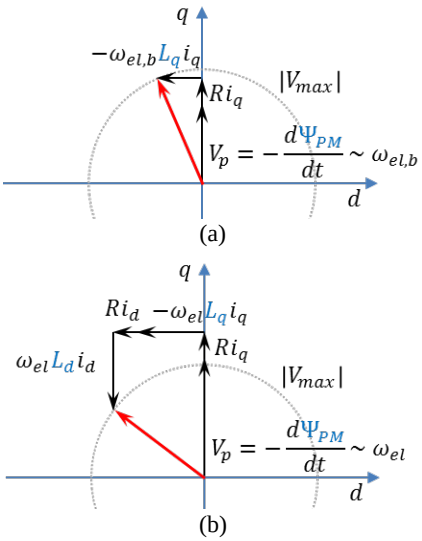

Figure 1: Phasor diagram of the PMSM: operation a) at base speed $\omega_{el,b} = p\omega_{mech,b}$ ($i_d = 0$) and b) at $\omega_{el} > \omega_{el,b}$ with field-weakening ($i_d < 0$).

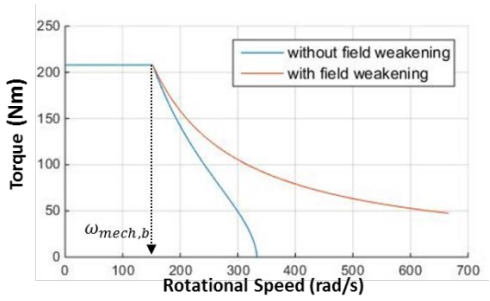

Figure 2: Example of a torque-speed diagram.

2. Motor

2.1 Setup and winding topology

The motor has a pole pair number $p = 5$ and $N_1 = 12$ stator slots in total. This yields a number of stator slots per pole per phase (SPP) $q = 0.4$ which is fractional according to equation (3) where $m = 3$ is the number of stator phases.

$$q = \frac{N_1}{2pm} \tag{3}$$

The stator winding is a concentrated two layer winding with one coil per tooth. It is designed so it can be pre-wound outside the stator and inserted afterwards. This is possible because of the characteristic shape of the coil cross-section which is shown in Fig. 3. In each phase, two neighboring coils are connected in series. These two coils are then connected in parallel with two others on the opposite side of the stator (Fig. 4). The three phases are connected at a star point (Fig. 5).

The rotor is equipped with ten buried magnets that are magnetized in alternative tangential directions. Circular holes are used as flux concentrators to direct the flux. This design leads to a rotor saliency (difference between L_d and L_q). By controlling the appropriate angle of the current space vector, the resulting reluctance torque can be used to improve the performance.

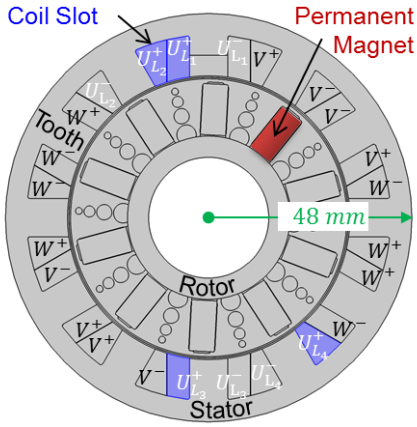

Figure 3: Components and electrical supply connections.

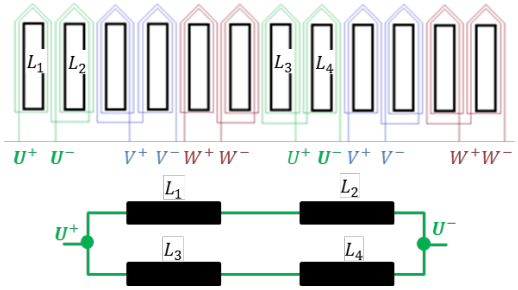

Figure 4: Winding topology.

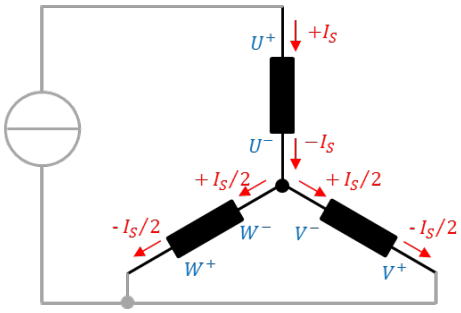

Figure 5: Coil and supply connection (cf. [9]).

2.2 Material

The material data for *cobalt steel Vacoflux 50* (stator, rotor, cf. Fig. 6) and *titanium* (rotor, cf. Fig. 6) are taken from [10]. In both cases, the electrical conductivity is reduced to a value of zero to suppress eddy currents. Some regions are modeled with the material properties of *Air* (cf. Fig. 6) and the data is taken from [10]. The permanent magnets *VACODYM 956 TP* are described by the constitutive equation:

$$\boldsymbol{B} = \mu_0 \mu_{PM} \boldsymbol{H} + \boldsymbol{B_R} \qquad (4)$$

The parameters in Eq. 4 are the remanent flux density $\boldsymbol{B_R} = (B_r = 0, B_\varphi = \pm 1.35, B_a = 0)T$ and the relative permeability $\mu_{PM} = 1.043$ taken from [11].

3. Use of COMSOL Multiphysics

All modeling is based on the *Rotating Machinery, Magnetic (rmm)* application mode. The rotor and stator are separate unions, which together form an assembly with the pair type: *identity pair*. In the physics node, different *Ampère's Law* domains are defined as summarized in Fig. 6. They differ regarding the constitutive relation for the magnetic field:

- Fig. 6a: nonlinear HB-curve
- Fig. 6b: $\boldsymbol{B} = \mu_0 \mu_r \boldsymbol{H}$ with $\mu_r = 1$
- Fig. 6c,d: cf. Eq. 4.

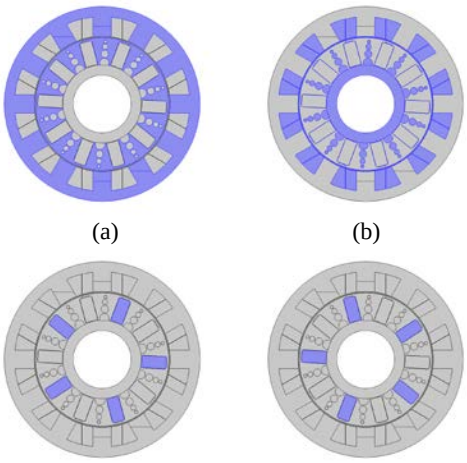

Figure 6: *Ampère's Law* domains: a) *Cobalt steel Vacoflux 50*, b) modeled as air, PM with c) $\boldsymbol{B_R} = (B_r = 0, B_\varphi = +1.35, B_a = 0)T$ and d) $\boldsymbol{B_R} = (B_r = 0, B_\varphi = -1.35, B_a = 0)T$.

Six *External Current Density* nodes are used to provide the supply currents according to the scheme in Fig. 5 (also cf. [9]). Furthermore, a *Pair Continuity* boundary condition is defined between the rotor and stator unions of the assembly. A *Force Calculation* domain is configured to determine resulting torque. Finally, a *Prescribed Rotational Velocity* domain is inserted to enable movement of the rotor.

With the described setup all modelling can be performed, even so not all nodes are enabled for all analyses simultaneously.

3.1 Location of *d*- and *q*-axis

A pre-condition for determination of the inductances L_d and L_q is the location of the *d*- and *q*-axis. The procedure suggested in [9] is applied. The motor is supplied with a constant current according to the scheme in Fig. 6. A parametric sweep over the relative angular position *phi* between rotor and stator is performed and the torque is calculated. The position for which the torque vanishes identifies the *d*-axis. From the simulation data of Fig. 7 $phi_d = 15.03\,°$ is obtained. The q-axis is found by rotating the rotor 90 electrical degrees:

$$phi_q = 15.03\,° - 90\,°/(p = 5) = -2.97\,°.$$

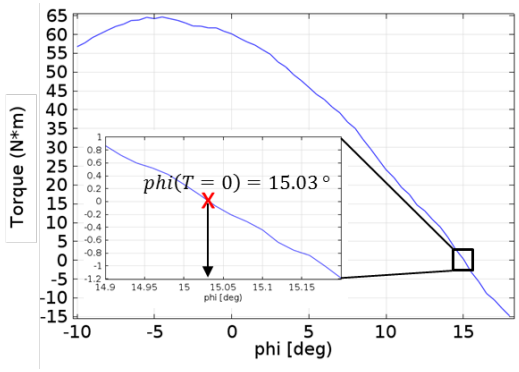

Figure 7: Torque versus relative angular position *phi* between rotor and stator. The inset shows a zoom to locate the *d*-axis at $T = 0$.

3.2 L_d and L_q inductances

The procedure for the inductance calculation will be exemplified for the L_d case. First, the geometry is fixed to the *d*-axis. Then a transient simulation for harmonic current supply is performed. The time-dependent magnetic flux density is obtained. Fig. 8 shows an example for a

certain point in time. The magnetic flux in tooth 1 can be determined by using the coupling integrating operator $intop$ (cf. Fig. 8):

$$\Phi_{tooth-1} = l_{Fe} \cdot intop(rmm.By). \quad (5)$$

In Eq. 5, $rmm.By$ is the y-component of the magnetic flux density (perpendicular to the integration path) and $l_{Fe} = 105\ mm$ is the out-of-plane thickness (z-direction). The tooth flux has an offset related to the impact of the permanent magnets. The flux contributed only by the coil current can be determined as [9]:

$$\Phi_{L1}(t) = \Phi_{tooth-1} - \frac{1}{T}\int_0^T \Phi_{tooth-1} \cdot dt \quad (6)$$

Similarly, the procedure is applied to calculate $\Phi_{L2}(t)$. Finally, the overall PMSM inductance $L_d(t)$ is obtained from:

$$L_d(t) = \frac{2}{3} \cdot n_{wind} \cdot \frac{(\Phi_{L1}(t)+\Phi_{L2}(t))/2}{I_s(t)/2} \quad (7)$$

with $n_{wind} = 10$ being the number of turns in the winding and $I_s(t)$ is the harmonic supply current (cf. Fig. 4,5). The factor $2/3$ results from the calculation of the overall inductance of the three components connected as shown in Fig. 5.

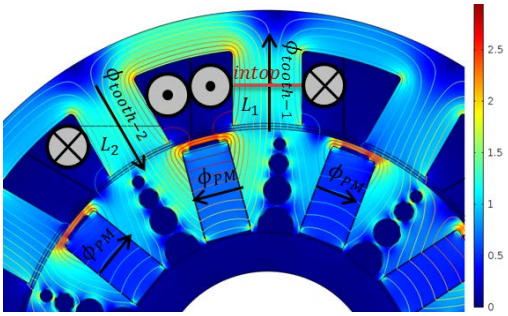

Figure 8: Simulated magnetic flux density for d-axis orientation. The coupling operator $intop$ is used to integrate the y-component of the magnetic flux density along the red line in tooth-1. The tooth flux follows with Eq. 5.

The procedure for determining $L_q(t)$ is similar with the exception of changing the rotor to the q-axis position. Finally, the exciting coil current can be substituted for time t to obtain the current dependency of the inductance. The resulting diagram is shown in Fig. 9.

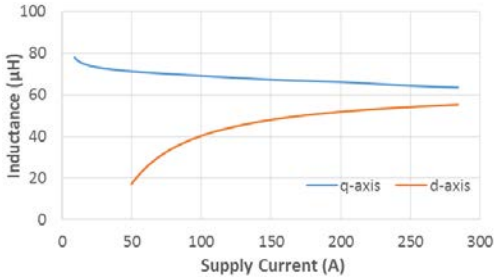

Figure 9: Calculated L_d and L_q inductances.

3.3 Voltage constant

In order to predict the motor behavior as illustrated by Fig. 1 the relation between the amplitude of the induced voltage $\hat{V}_p$ and the rotational speed is required [7]:

$$\hat{V}_p = \underbrace{\hat{\Psi}_{PM} \cdot p}_{k_n} \cdot \omega_{mech} \quad (8)$$

In Eq. 8, k_n is called the voltage constant. In order to obtain this parameter, the rotor is operated at ω_{mech}. The *Prescribed Rotational Velocity* physics node is configured accordingly. In addition, the model geometry is modified as shown in Fig. 10. Two explicit coil windings per inductance L_1 and L_2 are modeled. The induced voltage in one single winding (V_{L1} in L_1 and V_{L2} in L_2) is found by integrating the z-component of the electric field E_z over the cross-section with the area A_{wind}:

$$V_{L1} = \frac{l_{Fe}}{A_{wind}}\left(\int_{A_{1r}} E_z\, dA - \int_{A_{1l}} E_z\, dA\right),$$

$$V_{L2} = \frac{l_{Fe}}{A_{wind}}\left(\int_{A_{2l}} E_z\, dA - \int_{A_{2r}} E_z\, dA\right). \quad (9)$$

Eqs. 9 are implemented with coupling operators on the domains A_{1r}, A_{1l}, A_{2r} and A_{2l} (cf. Fig. 10).

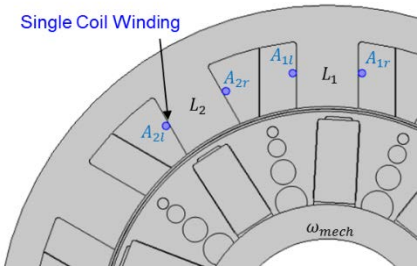

Figure 10: Model setup for calculating the voltage constant k_n.

The overall induced voltage V_p follows as:

$$V_p = n_{wind} \cdot (V_{L1} + V_{L2}). \qquad (10)$$

The simulated data in Fig. 11 is obtained for $\omega_{mech} = 1047\ rad/s$. The result can be used to extract the amplitude value $\hat{V}_p$. Finally, Eq. 8 can now be used to determine k_n.

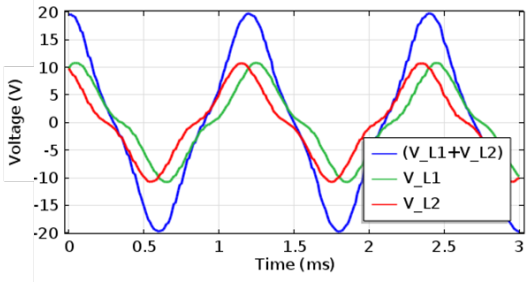

Figure 11: Simulated induced voltage for $\omega_{mech} = 1047\ rad/s$.

3.3 Torque transient behavior

Finally, the transient torque behavior is simulated. The *External Current Density* nodes are configured according to:

$$\text{U:} \quad J_z \cdot \cos(\omega_{el} \cdot t),$$

$$\text{V:} \quad J_z \cdot \cos(\omega_{el} \cdot t + 2\pi/3),$$

$$\text{W:} \quad J_z \cdot \cos(\omega_{el} \cdot t + 4\pi/3). \qquad (11)$$

The *Prescribed Rotational Velocity* node sets the rotor speed ω_{mech}. The angle $phi = -5\,°$ is selected to obtain maximum torque (cf. Fig. 7). Fig. 12 shows the results for varied current densities. At the rated value (J_{rc}, cf. Fig. 12) a torque of $T \approx (64 \pm 1)\ Nm$ is verified.

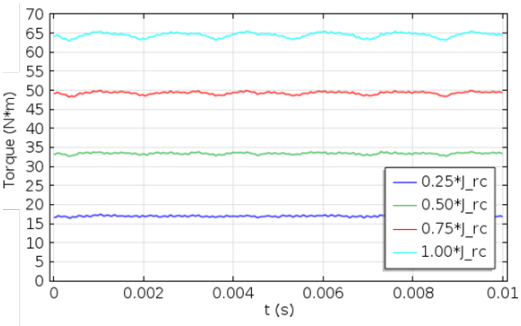

Figure 12: Torque transient behavior for different fractions of rated current density J_{rc}.

4. Conclusions

Simulation is a powerful tool, which was used during the design process of a permanent magnet motor for a Formula Student Electric racing car. Using the *Rotating Machinery, Magnetic* COMSOL application mode enables efficient model setup to extract the required parameters for the field-weakening motor control.

5. References

[1] *Formula Student Germany Magazine 2015*

[2] starkstromAUGSBURG, available from: <http://starkstrom-augsburg.de/> [30 July 2015]

[3] J. Güdelhöfer et al., Numerical Calculation of the Dynamic Behavior of Asynchronous Motors with COMSOL Multiphysics, *Proceedings of the 2012 COMSOL Conference*, Milan, (2012)

[4] Gerhard E. Stebner et al., Expert System for Synchronous Machines Based on COMSOL Multiphysics, *Proceedings of the 2011 COMSOL Conference*, Stuttgart, (2011)

[5] Charanjiv Gupta, et al., Finite Element Method as an Aid to Machine Design: A Computational Tool, *Proceedings of the 2009 COMSOL Conference*, Bangalore, (2009)

[6] S. T. Lee, L. M. Tolbert, "Analytical Method of Torque Calculation for Interior Permanent Magnet Synchronous Machines," IEEE Energy Conversion Congress and Exposition (IEEE), 2009, pp.173-177, 20-24 (2009)

[7] Austin Hughs, *Electric Motors and Drives: Fundamentals, Types and Applications*, Newnes, (2013)

[8] Tim Martin et al., Practical Field Weakening Current Vector Control Calculations for PMSM in Vehicle Applications, *International Battery, Hybrid and Fuel Cell Electric Vehicle Symposium*, (2013)

[9] W.L. Soong, Inductance Measurements for Synchronous Machines, *Power Engineering Briefing Note Series*, (2008)

[10] COMSOL material library

[11] Vacuumschmelze GmbH & Co. KG,: Rare Earth Permanent Magnets VACODYM • VACOMAX, Data sheet p. 39.